



# Battery materials for low-cost electric transportation

Kostiantyn Turcheniuk<sup>1</sup>, Dmitry Bondarev<sup>1</sup>, Glenn G. Amatucci<sup>2</sup>, Gleb Yushin<sup>1,\*</sup>

<sup>1</sup> School of Materials Science & Engineering, Georgia Institute of Technology, Atlanta, GA, 30332, USA

<sup>2</sup> Energy Storage Research Group, Department of Materials Science and Engineering, Rutgers University, North Brunswick, NJ, USA

This review considers key parameters for affordable Li-ion battery (LIB) – powered electric transportation, such as mineral abundance for active material synthesis, raw materials' processing cost, cell performance characteristics, cell energy density, and the cost of cell manufacturing. We analyze the scarcity of cobalt (Co) and nickel (Ni) resources available for intercalation-type LIB cathode materials, estimate the demands for these metals by transportation and other industries and discuss risk factors for their price increase within the next two decades. We further contrast performance and estimates costs of LIBs based on intercalation materials, such as lithium nickel cobalt manganese oxide (NCM), lithium nickel cobalt aluminum oxide (NCA), lithium iron phosphate (LFP) and other oxide-based cathodes and carbonaceous anodes, with those of LIBs based on conversion-type active materials, such as lithium sulfide (Li<sub>2</sub>S) and lithium fluoride/iron (Fe) and copper (Cu)-based cathodes and silicon (Si)-based anodes. Our analyses of industry data suggest that in the long-term the LIB price will be dominated by cost of the cathode materials. In addition, the cost contributions of manufacturing, overhead and inactive materials will be reversely proportional to the cell energy density. As such, we expect that to-be developed energy-dense conversion-type LIBs should be able to reach the \$30–40/kWh by around 2040–2050, while the intercalation-type LIBs will likely be 60% more expensive and sensitive to the Ni price variations. By analyzing the availability and costs of lithium (Li), sulfur (S), Si, fluorine (F), Fe and Cu we conclude that the lower cost, broader accessibility, much greater abundance, and improved health and safety aspects of employing conversion-type chemistries should warrant dedication of substantial efforts in their development. Furthermore, we predict that based on pure economics, the widespread introduction of zero carbon-emission transportation and sustainable energy sources is inevitable and independent on the winning LIB chemistry.

## Why Li-ion rather than other metal-ion rechargeable batteries

During the last 28 years the evolutionary improvements in lithium-ion battery (LIB) technologies increased LIB volumetric and gravimetric energy densities by over 3 times (from ~200 to over 700 Wh L<sup>-1</sup> and from 80 to 250 Wh kg<sup>-1</sup>, respectively) [1] and reduced cell price by up to 45 times (from over \$4500

kWh<sup>-1</sup> to \$100–250 kWh<sup>-1</sup>). As a result, LIBs mostly replaced other rechargeable battery technologies for most portable applications with the exception of lead-acid batteries [2]. Aqueous nickel-cadmium and nickel-metal hydride cells lost their market share due to LIB's substantially improved performance and lower cost [3]. Will Na-ion, K-ion, Mg-ion or Ca-ion be able to replace LIBs for ground electric transportation in the long run due to lower cost and larger reserves of Na, K, Mg and Ca compared to Li? The answer depends on how ion replacement may reduce battery pack-level cost. Battery pack cost is currently a decisive

\* Corresponding author.

E-mail address: Yushin, G. (yushin@gatech.edu)

factor for their use in electric vehicles (EVs) (provided, of course, that cell stability, specific energy and energy density meet the minimal requirements) [4,5]. The pack cost depends on (i) packing module design, cost and efficiency (which considers cooling requirements and pack complexity), (ii) cell energy density (in the units of Wh/L) because packs and battery management systems become more expensive if larger number of less energy dense cells of the same dimensions are utilized, (iii) the energy-normalized cell cost (in the units of \$·kWh<sup>-1</sup>). The energy-normalized cell cost depends on (a) the cost of cell materials (both active and inactive); (b) the cost of cell manufacturing; and (c) cell energy density (because larger number of the less energy dense cells and more materials need to be produced to attain the same energy). There is also the shipping costs and the cost of sales, R&D and profits. It has been estimated that replacement of Li by Na or other metals may reduce the automotive cell material costs by up to 1.5–3% without any changes in the cell manufacturing, depending on the price of Li and Cu [6]. Yet, so far, such replacements also reduce cell energy density by 15–40%, which, in turn, increases energy-normalized cell cost and battery management system cost to the levels where these novel technologies become not economical now and likely in the foreseeable future [6].

## Li-ion batteries in ground electric transportation

Fig. 1 illustrates the key factors that should be improved significantly to attain affordable electric transportation with LIB packs:

(1) mineral abundance for active material synthesis, (2) raw materials' processing cost, (3) cell performance characteristics and (4) module/pack design. Transportation already accounts for the largest portion of rechargeable batteries market and full electrification of ground vehicles is believed to be only a matter of time [7,8]. Currently, however, transportation sector is heavily dependent on carbon-based liquid fuels and one of the strongest contributors to the air pollution and increased CO<sub>2</sub> and CH<sub>4</sub> emissions, which resulted in climate change, increased probability of natural disasters and other undesirable outcomes [9]. As of 2020, world energy consumption in the transportation sector exceeded 3·10<sup>4</sup> TWh, which is ~20% of the total energy produced. Burning of fossil fuels in an increasing rate in the last century has urged a gradual transition to the renewable and less contaminating sources of energy, such as solar, wind, tides, waves and geothermal [10]. It also initiated a transition to battery-powered electric vehicles (BEVs) or fuel cell electric vehicles (FCEV) [11], with BEVs taking a significantly larger share of the market due to their better overall energy efficiency, higher power, lower cost and convenient recharging [12]. The LIB production world-wide is expected to exceed 1 TWh by 2028 [4] to satisfy the growing BEV demands and needs to grow further by substantially more than an order of magnitude to enable full electrification of ground vehicles. The future demand is typically speculated based on the projected cost reduction in LIB cells from the current \$100–250 kWh<sup>-1</sup> to below \$70–80 kWh<sup>-1</sup> [13], and the battery pack cost to fall below \$90–100 kWh<sup>-1</sup>.

77  
78  
79  
80  
81  
82  
83  
84  
85  
86  
87  
88  
89  
90  
91  
92  
93  
94  
95  
96  
97  
98  
99  
100  
101  
102  
103

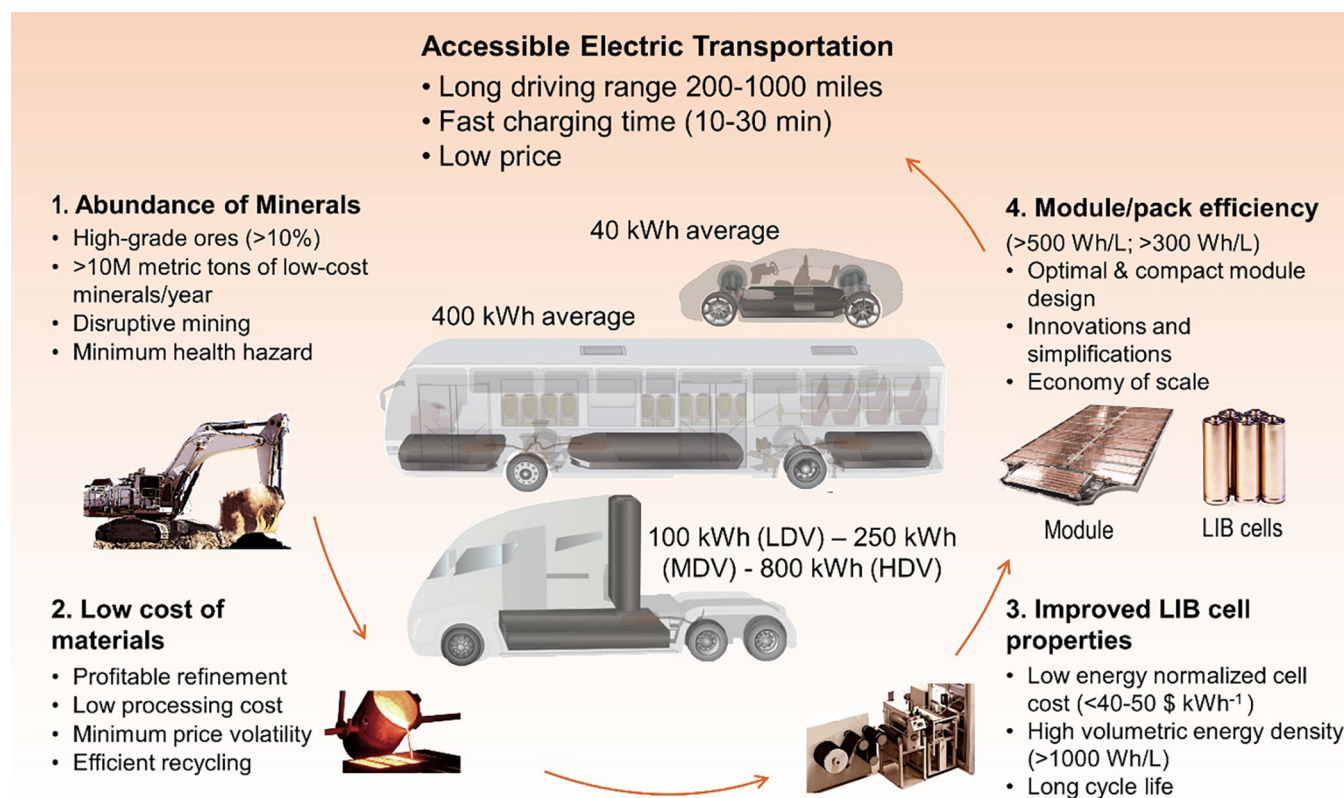


**FIGURE 1**

Key improvement areas for affordable electric transportation: (1) mineral abundance for active material synthesis, (2) low raw materials' processing cost, (3) high cell performance characteristics at reduced cost and (4) efficient module/pack design.

109 Reducing the pack cost to below \$40–50 kWh<sup>-1</sup> would greatly  
110 accelerate the transition to renewables beyond the initial  
111 projections.

112 However, such price reductions are not easy to attain and the  
113 improvements in the highest performance LIB energy density  
114 has been slowed down to a mere 1–2% per year as the technology  
115 matured, conventional intercalation-type active materials  
116 approached their theoretical limits and further reduction in  
117 thickness of current collectors and separators increased the risk  
118 of runaway reactions that might lead to spontaneous ignition  
119 [14]. Will it become feasible to achieve 2–5x LIB cost reduction  
120 with the economy of scale alone? Unlikely in the next many dec-  
121 ades because only moderate financial benefits could be attained  
122 with further increase in production volume once substantial  
123 scale has been reached [15]. Recent estimations that take into  
124 consideration both the scale and the cost of raw materials, even  
125 argued that the pack-level cost will unlikely be reduced to less  
126 than \$130 kWh<sup>-1</sup> [16] in the near future without subsidies unless  
127 fundamentally new active (Li-storing) materials replace conven-  
128 tional anodes and cathodes to increase cell-level energy density  
129 of BEV LIBs, while reducing total (active and inactive) materials  
130 costs (which already account for 50–65% of the LIB cell price).

### 131 Battery chemistries for electric transportation

132 Several conventional active cathode materials are currently being  
133 pursued for BEV LIBs: (i) high capacity/high voltage lithium  
134 nickel cobalt aluminum oxide cathode (NCA, currently com-  
135 monly LiNi<sub>0.8</sub>Co<sub>0.15</sub>Al<sub>0.05</sub>O<sub>2</sub>) or (ii) lithium nickel cobalt man-  
136 ganese oxide cathode (NCM, preferably higher capacity Ni-rich  
137 variants, such as NCM622-LiNi<sub>0.6</sub>Co<sub>0.2</sub>Mn<sub>0.2</sub>O<sub>2</sub> or more prefer-  
138 ably NCM811-LiNi<sub>0.8</sub>Co<sub>0.1</sub>Mn<sub>0.1</sub>O<sub>2</sub> [17]); (iii) lithium manganese  
139 oxide LiMn<sub>2</sub>O<sub>4</sub> (LMO) and (iv) lithium iron phosphate LiFePO<sub>4</sub>  
140 (LFP). Despite high costs of Ni and Co metals compared to Fe  
141 and Mn, the NCA and NCM-based LIBs and battery packs are  
142 known to be substantially cheaper than LMO- and LFP-based  
143 ones due to higher energy densities of the former. While higher  
144 capacity Co-free “NCA”, Co-free “NCM” and Li-rich “NCM” are  
145 being researched heavily [18], it is unclear if these could reach  
146 the automotive LIB performance requirements in the next dec-  
147 ade due to multiple known technical issues [17]. Furthermore,  
148 even upon success, development of such chemistries will still  
149 not reduce LIB cost sufficiently, but will reduce reliance on min-  
150 ing of Co which has a documented negative societal impact.

151 Can we expect lower cost of key raw materials to become a  
152 norm in the future? As we recently mentioned in our comment  
153 [19], such a scenario may be unlikely as well. The cost of Fe (in  
154 LFP) and Mn (in LMO) is already very low and rather stable  
155 and the growing battery demands will unlikely affect these.  
156 The situation with Co and Ni is gloomier. The increase in  
157 demand for the BEV LIBs has caused wholesale prices of Co to  
158 increase from ~22 \$/kg to ~36 \$/kg (with a temporary maximum  
159 of 95 \$/kg due to mismatch in supply and demand) over the past  
160 two years [20]. As a result, the cost of most cathodes increased by  
161 about 30–60% from Jan 2017 to Mar 2018 [21]. Note that both  
162 NCA and NCM cathodes typically comprise 6–12 wt. % Co and  
163 36–48 wt. % Ni. For example, moderate 75 kWh LIB utilizes  
164 ~100 kg of cathode material and thus requires 6–12 kg of Co

and 36–48 kg of Ni. Massive growth of the BEVs will require mil-  
lions of metric tons of Co and Ni, which should increase prices  
on these commodities, as we will discuss in detail further. Addi-  
tionally, market push for LIB cost reduction may have multiple  
undesirable outcomes if LIB chemistry does not change. For  
example, Amnesty International [22] and Bloomberg Technol-  
ogy [23] described the most outrageous exploitations of children  
and adult workers in Co mines in Africa and shocking levels of  
air, water and land pollution of natural graphite-mining villages  
in China, both endangering health and life of workers and their  
families. Small (artisanal) mines are particularly poorly regulated  
and often involve workers mining toxic Co by hands or using  
basic tools with little to none personal protection equipment  
to dig underground tunnels, and such mines account up to a  
fifth of African production in 2017 [23]. As such, we stress that  
the societal impacts of expanding mining operations to support  
BEV should not be negative relative to the potential positive  
gains of lower toxic and CO<sub>2</sub> emissions resulting from the elim-  
ination of ICE based transportation.

In this work, we analyze the availability, price volatility and  
sustainability of key materials to evaluate their potential for  
long-term BEV applications. We stipulate that the development  
and scale-up of ultra-high capacity alloying-type anode and  
conversion-type cathode chemistries based on abundant and  
inexpensive raw materials (such as Si, Fe and Cu, among others)  
to double LIB energy density is highly desired to exceed BEV LIB  
cost targets, to overcome the scarcity of Co and Ni reserves and to  
finally enable unobstructed and full transition to much cleaner  
BEVs.

### Available deposits of Co and Ni

Looking at the amount of metals present in Earth’s crust may  
lead to erroneous conclusions about their abundance and avail-  
ability because the cost of most metals is strongly influenced  
by their concentration in ore [24]. For example, the Earth’s crust  
contains approximately 0.7 Pt [25] (peta metric tons) of Co, how-  
ever, the commercially viable deposits of this metal are limited to  
only 25.5 Mt (million metric tons) [26] (Fig. 2a). Similarly, Ni’s  
content in the Earth’s crust is 2.1 Pt, the commercially available  
deposits of Ni are estimated to be 130 Mt (Fig. 2a) [25]. The sell-  
ing prices of materials inversely correlate with their concentra-  
tion in available deposits (Fig. 2b) [15,27], because lower  
mineral concentration increases the amount of the ore that must  
be processed and typically requires employment of additional  
capital-intensive processing technologies [28]. The progress and  
cost reduction in such technologies is rather slow.

Beginning of 2000s Co costs underwent strong growth due to  
the rapidly rising demands of the portable devices and battery  
EVs [26,29]. Pure Co or Co-containing salt deposits are not found  
in nature. Due to somewhat similar ionic radii of Co<sup>3+</sup> (0.525 Å)  
compared to Fe<sup>3+</sup> (0.645 Å) and Ni<sup>2+</sup> (0.69 Å), Co is mainly substi-  
tuting these metals and is found in more than 30 principal Co-  
bearing minerals [30,31]. The total terrestrial Co resources are  
estimated to be ~25.5 Mt [30,32], with: (i) ~1.38 Mt of the  
highest-grade ores (1.0–1.5 wt. %) [30]; (ii) ~4.84 Mt high-  
grade ores (0.3–0.9 wt. %), (iii) ~3.21 Mt medium-grade Co ores  
(0.2–0.3 wt. %) [30], (iv) ~5.75 Mt lower grade ores (0.1–0.2 wt.

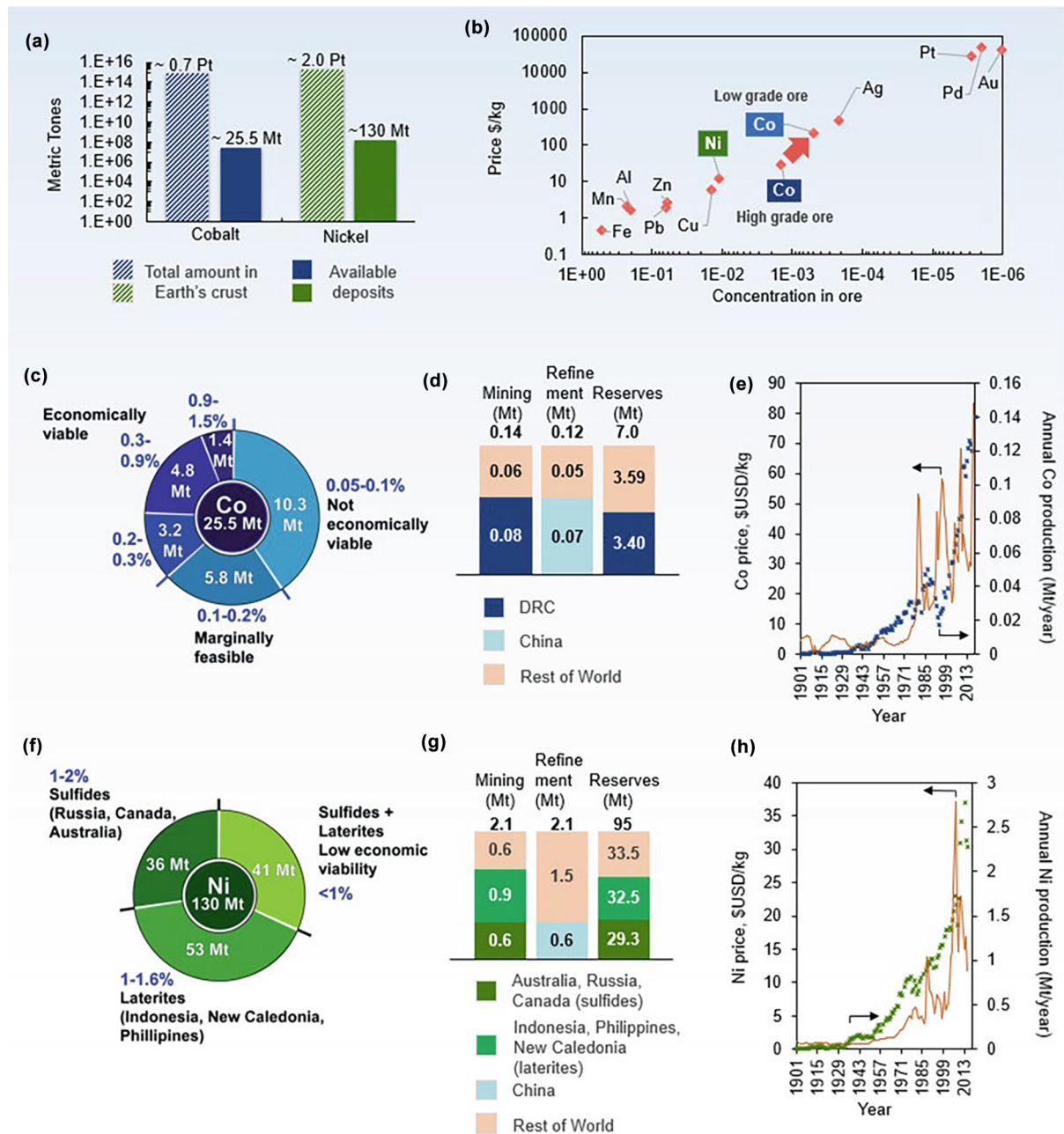


FIGURE 2

Resources of Co and Ni available for auto-LIB cathode materials [26]: (a) amount of Co and Ni available in Earth's crust compared to their terrestrial mining reserves; (b) dependence of metal prices on their concentration in the ore; (c) distribution of resources of Co by concentration and (d) country of origin; (e) historical prices for Co; (f) distribution of resources of Ni by concentration and (g) country of origin; (h) historical prices for Ni.

221 % and (v) ~10.3 Mt very low grade deposits (0.01–0.1 wt. %) 222 (Fig. 2c) [30]. Among these available terrestrial Co, ~7 Mt are eco- 223 nomically profitable for mining at recent prices [26], and a por- 224 tion of the ~8 Mt of marginal reserves may become 225 economically viable [33] with further advancements of mining 226 technologies in combination with Co price climb (Fig. 2c). Still, 227 the depletion of the high-grade Co ores should inevitably 228 increase prices of already rather expensive Co. High levels of 229 radioactive uranium in some of the remaining ores [34] will addi- 230 tionally contribute to substantially higher Co processing cost. In 231 comparison, the prices of metals which are contained in the

221 high-grade ores, such as Fe (20%) or Al (11%), will likely not 222 change considerably [35]. While the identifiable Co resources 223 on the seabed are massive (~120 Mt) [30], they will not be avail- 224 able to satisfy the growing EV demands because the seabed min- 225 ing is very expensive [36], and because the development of 226 suitable environmental policy regulations that protect the safety 227 for the deep ocean habitat will take decades [37]. 228

229 Other significant limitations of Co for EVs and other cost- 230 sensitive applications with relatively small profit margins are its 231 price volatility and its dependence on the Cu/Ni mining indus- 232 tries [38]. Indeed, nearly all Co is mined as a by-product of Cu 233

and Ni mining [30]. As such, independent increase in Co demand would unproportionally increase its mining cost. The intermittent shortage of Co supply or the accumulation of stocks when Co demand was weakened (e.g., induced by changes in the metallurgical industries) caused substantial volatility of Co prices (Fig. 2e) [39].

The uneven distribution of the Co-rich minerals in Earth poses yet another big risk [40]. Nearly 60% of Co mined in 2019 came from the Democratic Republic of Congo (DRC) [30], which possess majority of all commercially available Co deposits [33]. The lack of environmental legislation enforcement in Africa has caused the mines to have a significant negative impact on the overall health of the dwellers of neighborhoods adjacent to the Co production facilities [41,42]. The exposure to Co dust has been associated with adverse respiratory, pulmonary, and neurological diseases that lead to cancers and breathing difficulties, danger to unborn children and deaths to those exposed for prolonged time [43]. While public pressure to adopt better practices has led some companies to follow strict regulations to verify Co suppliers [44], many mines continue to employ problematic practices. China has gradually gained controls in the export of Co-containing ore from the DRC, becoming the world largest Co refinery (Fig. 2d) [40].

The rising costs of Co has pushed the LIB cathode producers to shift their attention to Ni-rich cathode materials with reduced Co content. However, the prevalence of Ni-rich cathodes to satisfy the grand demands of the future electric transportation may face similar challenges of price volatility and price increase. The commercially viable deposits of Ni have been estimated to be between 74 and 130 Mt [46] (Fig. 2f). In 2016, about 2.1 Mt were consumed by all industries with battery-related applications accounted for <10%. As the world will face the depletion of the rich (>1%) Ni ores in ~20 years, the increase in Ni prices may be inevitable.

Most of the world's Ni terrestrial resources are hosted in Ni laterites (70%) and sulfides (30%) [46] (Fig. 2f). Australia, Indonesia, and New Caledonia possess over 60% of total world's reserves of Ni laterites (Fig. 2f–g) [26]. The grade of the laterite ore depends on its composition with maximum grade 1.6% for oxide and clay laterites and 2.4–2.6% for Ni silicates [47]. Outstanding barriers to the development of lateritic-Ni is in high capital cost of processing facilities, stable oxide mineralogy, low Ni concentrations, high moisture content, large volumes of consumables, fewer opportunities for side-product recovery, very high energy requirements, and technical challenges of hydrometallurgical process [47,48]. Consumption of Ni by aerospace, batteries and stainless steel production industries rapidly deflates Ni ore grade (Fig. 2h). In addition, political factors (Indonesia, China, Russia) and Ni demand increases by aerospace (United States, China, Russia) may contribute to future price volatility (Fig. 2h).

Another important concern for the battery industry is that only Class 1 Ni (the high-purity Ni >99.8%; priced at ~35% higher than the reference LME prices [49]) is suited for battery production due to the ease of processing and low purification cost to produce nickel (II) sulfate ( $\text{NiSO}_4$ ), a LIB cathode precursor [50]. Refining Class 2 Ni (lower-class purity Ni <99.8% – ferromagnetic, or nickel pig iron, NPI) remains prohibitively expensive for LIBs [48]. Class 1 Ni is easier to produce from sulfite

deposits (via Ni carbonyl route), while Class 2 is mostly made from laterite deposits (via primary extraction to matte or ferromagnetic) [48,49,51].

Global car sales approached 80 M in 2019 [52]. In order to investigate the potential availability of Co and Ni resources, we have built a projection model for year 2025–2050 based on the demand by electric transportation industry, including (i) electric cars, (ii) busses and (iii) trucks. The number of electric cars was estimated based on the public announcements with 120 M per year by 2050 [53], the number of electric busses – 1 M per year by 2050, and the number of electric heavy-, medium-, and light-duty vehicles (HDV, MDV and LDV) – 2.4 M, 1.3 M and 25 M per year, respectively, by 2050 (conservative sub-50% battery electrification of busses and trucks). Fig. 3a shows the energy storage demand contributions, which are close to previous estimates [6]. For simplicity, we assumed that on average the EV LIB will be made with NCA cathodes with relatively low amount of Co (9.2 wt.%) and high Ni content (48.9 wt.%). We assumed a small (40 kWh) battery pack in an average car, 400 kWh in a bus and 100, 250, and 800 kWh in LDV, MDV, and HDV, respectively. We also assumed that electrification of trucks will be delayed till 2030 [54,55].

Without a change in the LIB chemistry, an immense amount of Co supply would be needed to satisfy the annual transportation demand: ~0.32 Mt by 2030 rapidly growing to 0.76 Mt by 2040 and to 1.3 Mt by 2050 (Fig. 3b, c). The demands for Co use in magnets [56] and superalloys [57] will also likely experience growth. With current Co mining capabilities of less than ~0.15 Mt per year, the industry would need to increase fivefold by 2040 to keep up with the demand (Fig. 3c). If we limit ourselves to 9.2 Mt of “economically viable” Co reserves then these would be exhausted by early 2030–35 (Fig. 3c), forcing the price increase to open up “marginally feasible” reserves (Fig. 1c). Increasing the rate of recycling will help, but it cannot contribute enough due to rapidly rising market [58]. The situation with Ni is slightly better – the EV demands would exceed feasible mining from the “currently economically viable” reserves by ~2040 and surpass unsustainable 8 Mt per year by 2050 (Fig. 3d). Note that we optimistically considered both Class 1 and Class 2 Ni, which makes our estimations to be “best case” scenarios and doubling the Ni prices may be needed to initiate investments in the currently “marginally feasible” reserves to catch up with the expected demand. Multiple other factors may contribute to the volatility of Co and Ni prices (Fig. 3e).

### Costs of Co/Ni based intercalation cathodes

The NCM production commonly relies on the formation of the composite hydroxide from a mixture of  $\text{MnSO}_4$ ,  $\text{CoSO}_4$  and  $\text{NiSO}_4$  in a basic solution containing NaOH and  $\text{NH}_3$  [50]. The composite hydroxide is then annealed in the presence of LiOH or  $\text{Li}_2\text{CO}_3$  at temperatures of 700–1000 °C, which leads to the transformation of hydroxides and carbonates to oxides [59]. Alternatively, corresponding carbonates or hydroxides of the transition metals can be formed separately from the corresponding sulfates. Then dried carbonate precursor powders are lithiated with LiOH or  $\text{Li}_2\text{CO}_3$ . The raw materials contribute to 71–73% of the NCM price (~24.5 \$·kg<sup>-1</sup> or 0.12 \$·Ah<sup>-1</sup> for NCM811). Like

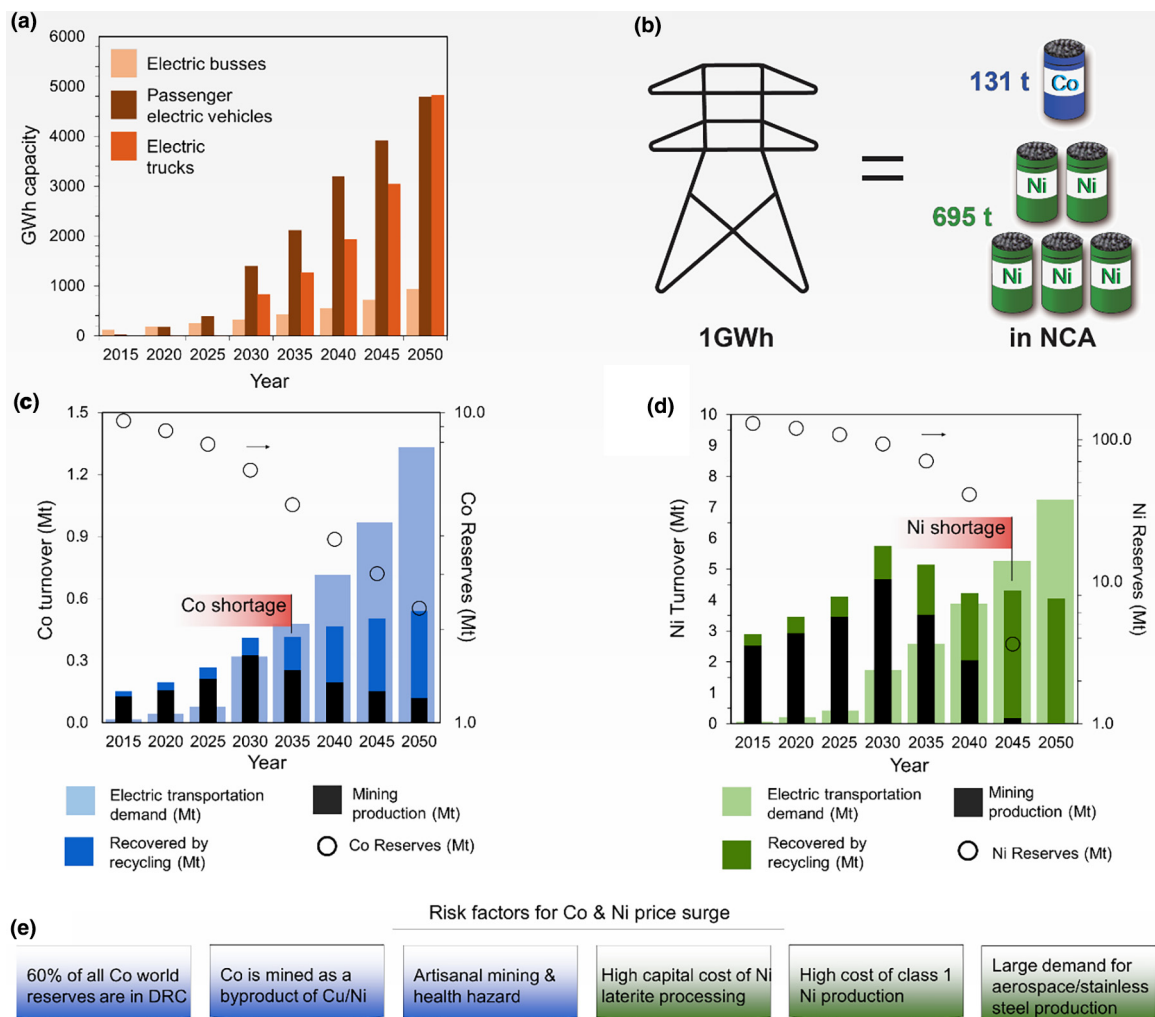


FIGURE 3

Expected demands for batteries and intercalation-type cathode materials: (a) battery capacity needed to satisfy gradual electrification of ground transportation; (b) approximate amounts of Ni and Co in intercalation-type LIB cathodes need to provide 1 GWh of energy storage; (c and d) expected demands for Co and Ni and the corresponding exhaustion of economically viable reserves; (e) key risk factors for Co and Ni price increase.

NCM, NCA is synthesized via co-precipitation [60]. The process of making NCA particles is only slightly more complicated and the raw materials contribute to  $\sim 70\%$  of the NCA price ( $\sim 26$   $\text{\$}\cdot\text{kg}^{-1}$  or  $0.12$   $\text{\$}\cdot\text{Ah}^{-1}$ ).

### Cost of metal fluorides cathodes and available reserves of S, Cu and Fe

In an ideal case, LIB cathodes should both rely on lower-cost, broadly available metals and offer higher cell-level volumetric energy density in order to reduce cell and pack manufacturing costs and the energy-normalized costs of inactive materials (since all of these depend on the number of cells that needs to be made for an EV). Higher volumetric LIB energy density may originate either from higher volumetric capacity of the electrode materials or from higher average voltage. Both bring their own challenges. For example, selecting a chemistry to increase maximum charge to 4.6–5.0 V induces significant electrolyte oxidation (gassing) and corrosion (degradation) of both the cathodes and conductive carbon additives [61] during storage in a fully charged state [62],

particularly at elevated temperatures, which is in conflict with the need to attain a high cycle stability (1500+) and a long calendar life (10 years+) in BEV cells. High voltage operations additionally trigger stricter requirements on purity and dryness of all the cell components and the use of more expensive electrolyte solvents, which increases cell cost. High voltage spinel, such as  $\text{LiMn}_{1.5}\text{Ni}_{0.5}\text{O}_4$  (LMNO) [63] and olivine  $\text{LiCoPO}_4$  (LCP) [64],  $\text{LiNiPO}_4$  (LNP) [65] and others [66] offer relatively moderate (compared to 210–220 mAh/g in modern NCA) theoretical gravimetric capacity of 147 mAh/g (LNO) and 167 mAh/g (LCP and LNP), while olivines in addition rely heavily on Ni and Co and suffer from  $\sim 20\%$  lower density, which further reduces their volumetric capacity. Unfortunately, only a few options exist for increasing volumetric cathode capacity of intercalation cathodes beyond that of NCA or Ni-rich NCM (e.g., up to 970–1050  $\text{mAh}\cdot\text{cm}^{-3}$  at the particle level) [67,68]. For example, while a recent report on leveraging reversible  $\text{Mn}^{2+}/\text{Mn}^{4+}$  double redox couple into Li-excess cathodes  $\text{Li}_2\text{Mn}_{2/3}\text{Nb}_{1/3}\text{O}_2\text{F}$  and  $\text{Li}_2\text{Mn}_{1/2}\text{Ti}_{1/2}\text{O}_2\text{F}$  attained impressive 260–300  $\text{mAh}\cdot\text{g}^{-1}$  specific capacity

for cycling within 1.5–5.0 V vs. Li/Li<sup>+</sup>, its volumetric capacity (900–1050 mAh·cm<sup>-3</sup> at the particle level) did not exceed that of the state of the art NCA and NCM, while its average discharge voltage was over 0.5 V lower [69], leading to lower volumetric energy density. Furthermore, the need to charge to a very high potential and discharge to a very low potential in order to access such a high capacity induced instability in the cathode electrolyte interphase (CEI) and other uncontrolled side reactions (CO<sub>2</sub> release) leading to rapid cell failure [69,70].

With the lack of viable options in the intercalation compounds, we must likely look at a more “revolutionary” conversion-type cathode material chemistry to find sustainable solutions for lower-cost BEV transportation. The name “conversion” originates from the difference in the Li ion storage mechanism, where instead of reversibly intercalating Li ions in the interstitials of the crystal structure with no breakage of chemical bonds, electrochemical reaction with Li ions in conversion-type electrodes proceeds *via* a solid state conversion reaction, where crystal structure, material properties and chemical bonds change dramatically [71–76]. We would like to clarify that here we use a rather broad definition for the conversion reactions, that covers both chemical transformation and “true” conversion reactions, which, in turn, include displacement reactions. Out of various conversion-type cathodes, S (or Li<sub>2</sub>S in the lithiated state) and metal fluorides (primarily CuF<sub>2</sub> and FeF<sub>3</sub> or 2LiF/Cu and 3LiF/Fe in the lithiated state) stand out by offering particularly high theoretical volumetric capacities (1533–2196 mAh cm<sup>-3</sup> at the particle level) while attaining relatively high discharge potential [17,75,77–79]. Sulfur–lithium (S–Li) cells have already been used in unmanned air vehicles and now become of the most extensively studied chemistries [80,81]. From the low-cost and broad availability points of view all three S, Cu and Fe with cost of ~0.05 \$·kg<sup>-1</sup>, ~6.4 \$·kg<sup>-1</sup> and ~0.6 \$·kg<sup>-1</sup> and with economically viable reserves of 5 Bt, 720 Mt and 230 Bt, respectively, for S in volcanic deposits and associated with hydrocarbons and for Cu and Fe in high grade 1–30% ores [26], are attractive materials for batteries. Due to major research efforts already devoted, successful commercialization of S may come first. Yet our calculations demonstrate that MF<sub>x</sub> materials have a higher potential to reduce cost long-term than S. This is due to higher theoretical potential vs. Li/Li<sup>+</sup> and higher volumetric capacities than S. For example, in the lithiated state MF<sub>x</sub> offer 2002 mAh cm<sup>-3</sup> (FeF<sub>2</sub>) and 2196 mAh cm<sup>-3</sup> (FeF<sub>3</sub>) vs. 1935 mAh cm<sup>-3</sup> for S, thus approaching or exceeding that for pure Li (2062 mAh cm<sup>-3</sup>). The challenges and advantages of S (Li<sub>2</sub>S) cathodes have been covered in multiple excellent review articles [82–84] and will thus be omitted here.

Fig. 4 focuses on synthesis routes for the formation of non-lithiated (CuF<sub>2</sub>, FeF<sub>3</sub>, or MF<sub>x</sub>) or lithiated (2LiF/Cu and 3LiF/Fe or xLiF/Fe) metal fluorides. A common fluorine (F) source for synthesis of MF<sub>x</sub> is hydrofluoric acid (HF) (Fig. 5b), which could be handled economically at a very large scale in spite of being extremely dangerous [85]. HF (0.7 \$·kg<sup>-1</sup>) is typically produced from cheap (0.1 \$·kg<sup>-1</sup>) fluorspar mineral (CaF<sub>2</sub>) (Fig. 4a) [86], the economic reserves of which provide ~250 Mt<sub>F</sub> [87]. Other fluorine-based minerals, such as fluoroapatite (Ca<sub>5</sub>(PO<sub>4</sub>)<sub>3</sub>F), can also be used, which adds ~600 Mt<sub>F</sub> [86]. One example of a synthetic pathway for FeF<sub>3</sub> involves treatment of an iron precursor (e.g., nitrate (III) nonahydrate (Fe(NO<sub>3</sub>)<sub>3</sub>·9H<sub>2</sub>O) [88] or carbonate or

chloride or alkyls [89], etc.) with ~40% aqueous HF solution (Fig. 5b, d). A more expensive ammonium fluoride (NH<sub>4</sub>F; 1.3 \$·kg<sup>-1</sup>) could similarly be used [90]. Most importantly, because metallurgical industries utilize HF for surface purifications [91] producing enormous amounts of fluorinated solutions of Fe and Cu metal salts as waste products [91,92], (0.65 Mt/year of sludge in China alone [93]), such wastes could be used as negative-cost starting materials for the effective conversions to FeF<sub>3</sub> and CuF<sub>2</sub> [94]. Alternatively, fluorine-containing superacids, such as hexafluorosilicic acid [95] (H<sub>2</sub>SiF<sub>6</sub>, 1\$·kg<sup>-1</sup>, commonly used in water purification and manufacturing of aluminum [86] and produced as a byproduct of HF synthesis), may be utilized instead of HF (Fig. 5b, d) [96,97]. Gas phase fluorination of various organic or inorganic metal salt, carbide, nitride, hydride, oxide or pure metal (nano)particles may be effectively utilized for improved morphological control in FeF<sub>3</sub> or CuF<sub>2</sub> synthesis (Fig. 5b, d) [98,99]. These processes require only 100–400 °C heating [100], much lower than that involved in NCM or NCA syntheses. Common examples of gaseous F sources include various fluorine-containing gases (such as NF<sub>3</sub> or BF<sub>3</sub>) or vapors of fluorine-containing organics [95]. Synthesis of xLiF/M may involve chemical or electrochemical lithiation of the corresponding metal fluorides. As an alternative to lithiation, CaF<sub>2</sub> and LiCl can be used as starting materials for (nano)LiF synthesis directly in the water/alcohol solution due to its low solubility (Fig. 5h–g). Multiple sources of inexpensive gaseous Cu and Fe precursors are available as well (Fig. 5f).

## Challenges and advantages of metal fluoride cathodes

Somewhat similar to S and Li<sub>2</sub>S [82,83], MF<sub>x</sub> cathodes currently exhibit several challenges which still need to be systematically studied and resolved [101]. These include: (i) improving kinetics of electrochemical reactions, (ii) preventing localized mechanical failure due to volume changes, and most importantly (iii) preventing dissolution of M or F ions during cycling [102]. We expect that formation of nanocomposites or core–shell particles (nanoconfinement) (Fig. 4) may be needed to overcome these limitations. Indeed, nanoconfinement of metal fluorides in elastic matrix materials was shown to greatly reduce the dissolution of transition metals during cycling, accommodate volume changes and increase cycle life to 1000 cycles at high rates [102,103]. Precise control over the size of the MF<sub>x</sub> nanoclusters in such composites may be attained, for example, by the infiltration of MF<sub>x</sub> precursors into porous hosts with pre-determined pore size distribution followed by heat-treatment [104], or by carbonizing a solution-precipitated mixture of the MF<sub>x</sub> and matrix materials precursors [103,104]. An intimate connection of active material with electronically conductive C matrix enables uninterrupted supply of electrons to the electrochemical reaction sites (even if M and LiF clusters separate over time) for fast charge rates and near-theoretical capacity utilization. The use of core–shell architectures was shown to further enhance stability of such cathode materials [99]. The fundamentals of the electrochemical reactions in MF<sub>x</sub> systems, however, are still understood incompletely. The exact structural atomic rearrangements taking place during charge or discharge and their dependence on the crystal

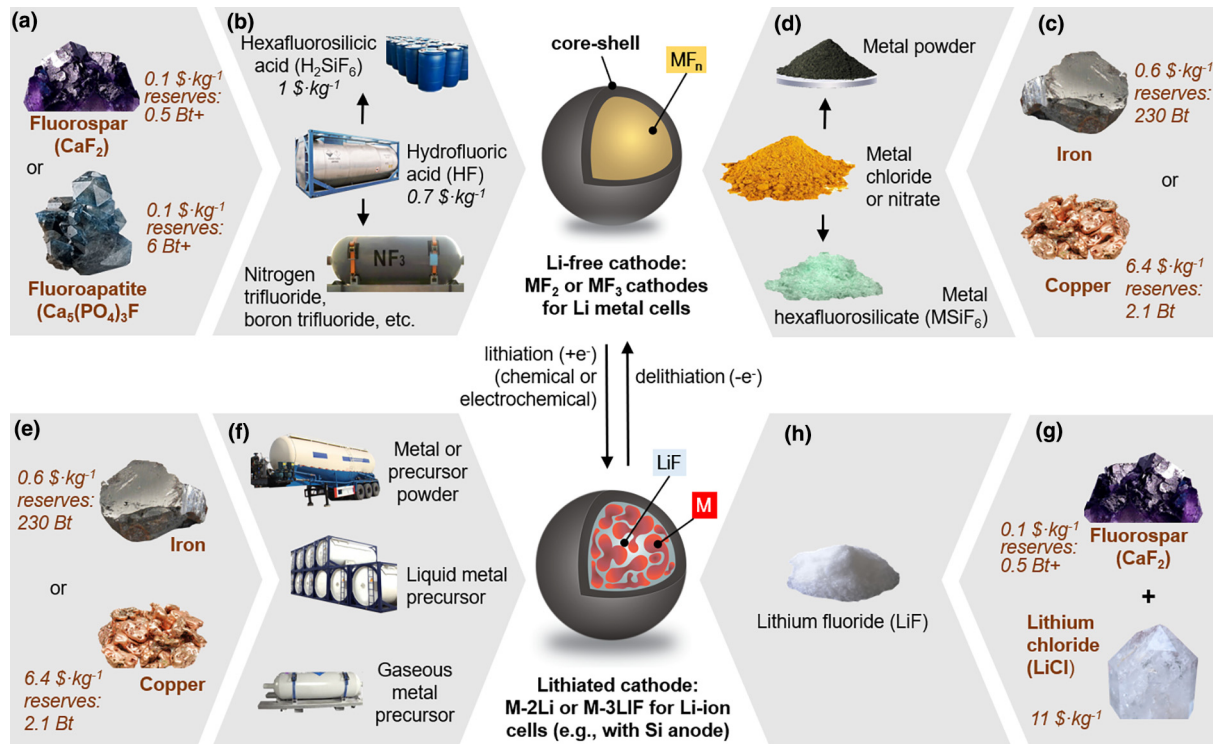


FIGURE 4

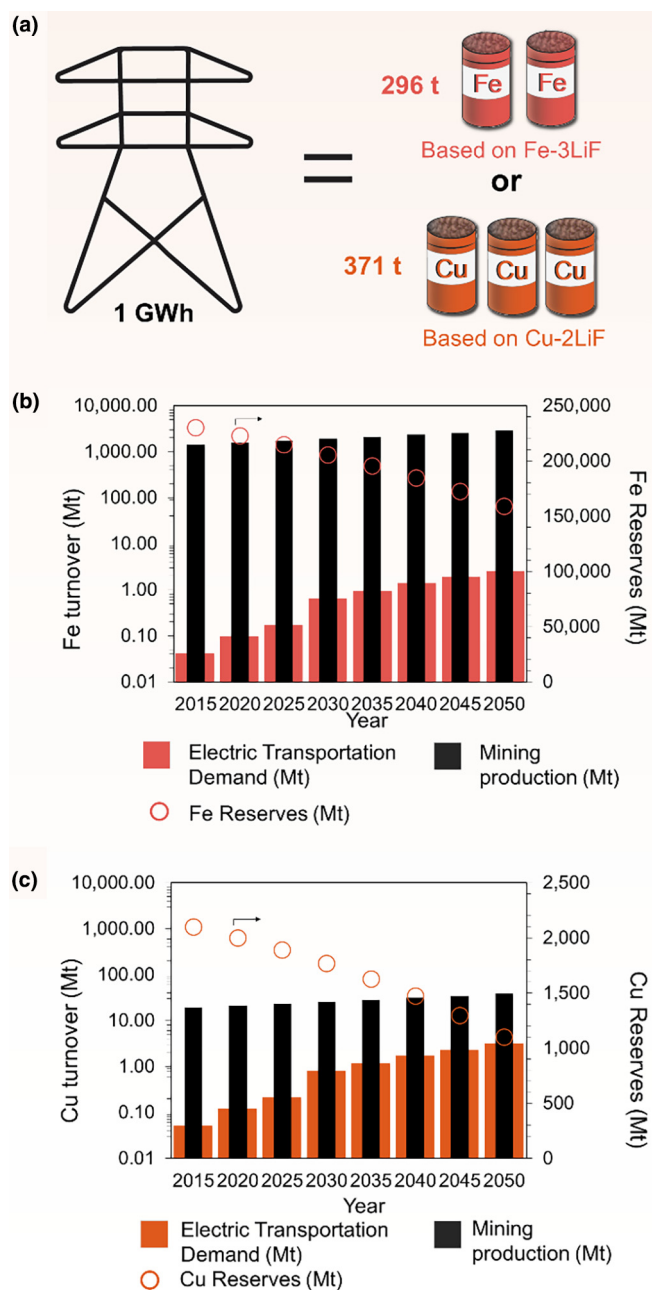
Example minerals for iron and copper fluoride cathodes and their reserves and typical prices: (a), typical fluorine-containing minerals used for the formation of (b) HF, which may be further transformed into liquid or gaseous fluorine sources; (c and e) iron and copper metals; (d and f) metal and metal precursors; (g) precursors for (h) LiF.

structure, size of the M or  $\text{MF}_x$  clusters, temperature, internal stresses, physical confinement, the properties and proximity of the electrolytes and their composition, among many others remain the subject of debates [105]. The contributions to the voltage hysteresis at different stages of the reaction also remain controversial [106]. The structure, composition, morphology and the formation mechanisms of the cathode electrolyte interphase (CEI) layers on the surface of active particles in contact with electrolyte need to be better understood and carefully optimized [99]. The use of alternative (e.g., solid or ionic liquid) electrolytes or tough and robust shells on the surface of the composite particles to assist in a stable CEI formation and metal-ion dissolution prevention show promises and should be further explored [102,107,108]. Holistic experimental approaches that include synthesis of precisely controlled materials [109–111] accompanied by various modeling efforts [112–114] in combination with some of the most advanced characterization (high-resolution transmission electron microscopy, high-resolution electron energy loss spectroscopy, high-resolution energy dispersive spectroscopy, electron diffraction, high-resolution X-ray diffraction and pair distribution function analyses, X-ray absorption spectroscopy, solid-state nuclear magnetic resonance spectroscopy, among others) will likely be needed to clarify the plethora of open questions [115]. Still, the authors are confident that with further efforts the synthesis, characterization, and modeling tools that are now available to scientists and engineers will enable one to resolve the present scientific and technological challenges to produce and scale commercially

viable conversion-type cathodes. For massive adoption of fluoride cathodes, however, their processing cost at scale should be sufficiently low (3–6 \$·kg<sup>-1</sup>). In addition, the total volume fractions of inactive components in the composites should be kept to a minimum (preferably to 5–16 vol. %) to maximize the cathode capacity. Considering the prices of combined raw materials (Cu or Fe, F, Li for the lithiated cathode versions), the final cathode costs would be in the 12.5–18.5 \$·kg<sup>-1</sup> (or 0.025–0.042 \$·Ah<sup>-1</sup>) range for  $x\text{LiF}/\text{M}$  cathodes, if metallurgical wastes are not used.

### Anode materials considerations

Three chemistries of anodes are considered for high-energy BEV LIB cells: (i) intercalation-type carbons (incumbent), (ii) conversion/alloying type Si and (iii) Li metal. All three offer low Li insertion potential to maximize cell voltage, while Si and Li additionally offer much higher gravimetric and volumetric capacities (~3 times higher volumetric and 10 or more times higher gravimetric capacities than that of the graphite at a particle-level when considering a charged and thus fully expanded state). We would also like to emphasize that due to the realistic need to produce electrodes in moisture-containing (e.g., regular air) environment (for low production costs, critical for EVs) and because of the extremely high reactivities of lithiated C, lithiated Si and Li metal with water, all these anodes likely need to be produced in a fully discharged (Li-free) state prior to assembling into cells.

**FIGURE 5**

Maximum demands for Cu and Fe in MF-based LIBs: (a) amounts of Fe and Cu in conversion-type LIB MF cathodes needed to provide 1 GWh of energy storage; (b) and (c) maximum demands for Fe and Cu as a fraction of their mining productions.

### Cost and available reserves of graphite

The low volume changes during insertion of Li ions into C (6–12 vol. %), its broad availability, low cost for sufficiently high purity (0.5–15 \$·kg<sup>-1</sup>), high electrical conductivity, high Li<sup>+</sup> mobility, reasonable volumetric capacity (~650–700 mAh·cm<sup>-3</sup> at the particle level) and low de-intercalation potential made C the material of choice for LIBs [116]. A portion of C in commercial LIB anodes is synthetic [117] and typically produced from massively available coal-tar pitches and petroleum coke (Fig. 6b) [118]. The reserves of the natural graphite are estimated at 300 Mt (Fig. 6a)

[26]. Unfortunately, the cost cutting during mining resulted in major workers' safety violations in graphite mines, where graphite dust was found to cover entire villages, damaging crops and belongings at homes and polluting drinking water [119]. The link between the exposure to graphite dust and pulmonary disease has been clearly established [120,121].

### Cost, available reserves, and material properties of Li for Li-ion, Li-metal and Li-air batteries

Li is a critical component of LIB cathodes. In addition, using Li foils or plating pure Li metal during charging may look attractive from the energy density perspective owing to high volumetric capacity of pure Li metal (2062 mAh·cm<sup>-3</sup>). Unfortunately, in the view of the authors it is highly unlikely that conventional BEV LIBs would utilize Li plating due to safety risks associated with the formation of Li dendrites, which may create thermal runaway-inducing internal short circuits, especially at the desired high areal current densities (4–20 mA·cm<sup>-2</sup>) [122]. Achieving homogenous, smooth and dense morphology of the plated Li metal and the stability of the solid electrolyte interphase (SEI) on its surface is extremely challenging in liquid electrolytes [123,124]. Despite major world-wide efforts during the last 20 years, without the use of excess Li and excess of electrolyte only 80–90% of capacity could so far be retained in 100 cycles or less [123]. The use of pillars or other three-dimensional (3D) structures on current collectors may enable lower surface-normalized plating currents (which are advantageous for smoother Li plating) [125,126], but at the expense of reduced volumetric anode capacity, higher first cycle losses, higher costs and other limitations, likely unpractical for low-cost and robust manufacturing of LIBs for transportation. The development and use of suitable solid state electrolytes (SSEs) offers a strategy to significantly reduce side reactions on the Li surface, but at the expense of much higher fabrication costs and reduced gravimetric performance [127]. Indeed, stability of the SSE/Li system depends on the chemical and physical uniformities of the anode current collector, the SSE electrolyte, and the deposited Li, which are expensive and challenging to attain [128]. Since plating of Li metal changes volume in the cell, it generates stresses that may lead to the SSE failure (e.g., through Li dendrite penetration or crack formation and propagation within the SSE) if these stresses are concentrated on various nonuniformities [128,129]. Unfortunately, most ceramic or glass/ceramic electrolytes contain small pre-existing defects, such as grain boundaries, pores, impurities, inclusions, dislocations, and others, unless expensive vapor deposition techniques are utilized for their production [130] (as in the case of LiPON SSE). In addition, small variations in the SSE properties (e.g., the presence of grain boundaries or voids or chemical nonuniformities or orientation-dependent conductivity) or variations in the properties of the current collector or even the contact between the SSE and current collector may lead to the presence of dangerous defects and low production yield [130]. While good cycle life in a few tiny research cells (0.5–10 cm<sup>2</sup>) with extremely uniform SSEs has been demonstrated at low or moderate current densities (0.02–3 mA·cm<sup>-2</sup>) [131], preventing formation of cell-killing defects in an automotive battery with ~500 m<sup>2</sup> of the high areal

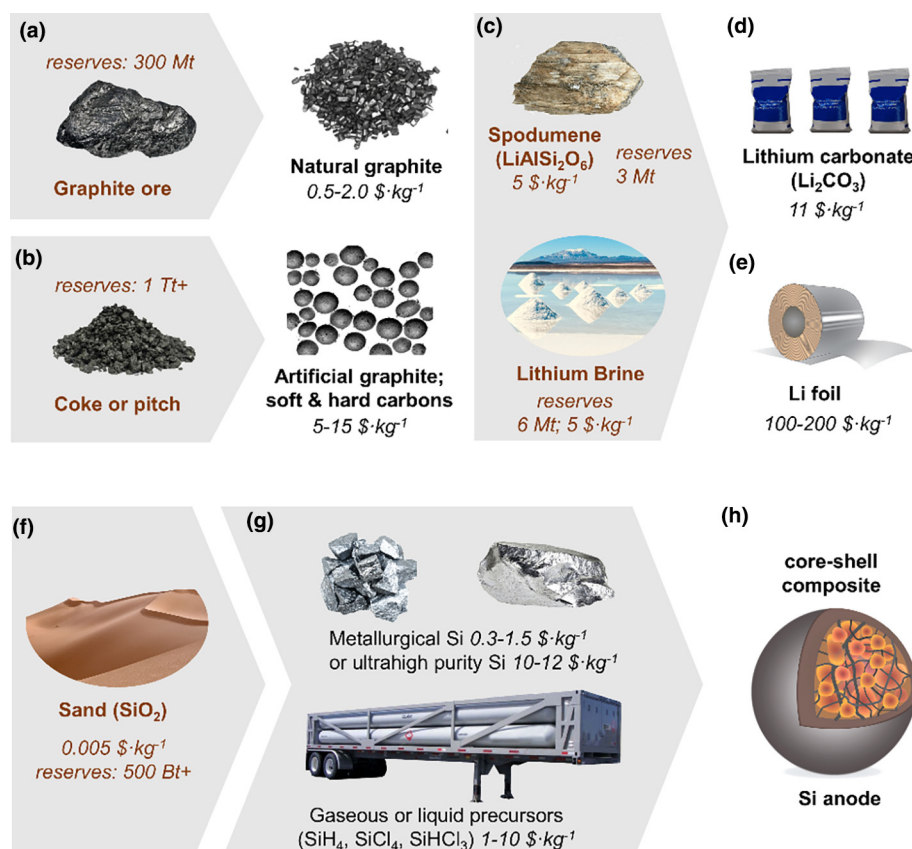


FIGURE 6

Example minerals for carbon, Li and Si anodes and their reserves and typical prices: (a and b) precursor courses for natural and artificial graphite; (c) common minerals for Li carbonate (for use in cathodes) or Li foil anodes; (f) sand used for (g) solid, liquid or gaseous Si precursors for use in (h) Si anodes.

capacity electrodes subjected to fast charging (4–20 mA·cm<sup>-2</sup> current density) is dramatically more challenging. From the point of view of the authors, successful approach would likely require the use of precise, semiconductor-grade equipment and processes that are orders of magnitude too expensive for BEV batteries.

One popular class of conversion-type cathode materials we ignored in our previous discussion is a so-called “oxygen” or “air” cathode in the form of Li<sub>2</sub>O<sub>2</sub> active material dispersed on a porous substrate for aprotic or SSE electrolytes or LiOH for aqueous electrolytes [79,132,133]. Let us explain the reasons we don’t consider such a chemistry for BEVs. We will start by emphasizing that so far there are no aprotic electrolyte solvents identified that are suitable for Li-Li<sub>2</sub>O<sub>2</sub> cell chemistry, and the deep fundamental reasons of such a severe limitation have been nicely summarized in a recent review article [134]. To prevent irreversible chemical reactions of a Li metal anode with a dissolved O or water or other species, the Li anode needs to be covered with a SSE protective layer [134]. If Si anode is used instead, the same protective surface layer still needs to be deposited [134]. The SSE layer on the Li anode is also needed to prevent Li dendrite formation and growth [135]. However, as we previously discussed, we don’t believe that the formation of suitable-quality SSE is realistic for severely price-constrained BEV applications. Due to uncontrolled and undesirable contaminations in air (carbon dioxide, moisture, etc.), the O<sub>2</sub> released during charge and

consumed during discharge likely needs to come from an O<sub>2</sub> gas cylinder, which complicates BEV battery design and increases its weight and volume (as it does for commercial nickel-hydrogen cells with a “hydrogen” cathode). The future development of inexpensive, highly penetrable by O<sub>2</sub> and yet highly-selective O<sub>2</sub> membrane could be desirable for “oxygen” cathodes [136], but is also extremely challenging. Furthermore, conventional cost-efficient automotive cells are relatively large and multi-layered. In contrast, academic studies on “oxygen” cathodes are conducted on single-layer cells where oxygen comes in/out from the top cathode layer to provide reasonably fast O<sub>2</sub> diffusion. In commercial cells this is unrealistic as the packaging material would consume too much volume and contribute to too high of a cost. Yet, the diffusion of O<sub>2</sub> from the sides of conventional dense cells would also be unrealistically long to provide reasonable power or charging rate. This complicates cell design by the need to introduce gas diffusion layers, further increasing cell cost and reducing its energy characteristics. When compared to intercalation-type or other conversion-type cathodes, the “oxygen” or “air” cathodes need to comprise finely distributed electrocatalyst and be dramatically more porous compared to allow for efficient O<sub>2</sub> diffusion, while preventing clogging of the pores by the discharge products [137]. The volume taken by such a high porosity filled with electrolyte as well as the catalyst particles and catalyst support, severely minimizes the volumetric capacity of the “oxygen” cathodes. As a result,

when compared to both  $\text{Li}_2\text{S}$  or  $x\text{LiF/M}$  cathodes, the  $\text{LiOH}$  cathodes offer lower volumetric and gravimetric energy density (as previously estimated even when using extremely favorable for oxygen cathode assumptions with zero volume budget for the gas diffusion layer in a unit stack [78]). While the cost of the “oxygen” active material ( $\text{LiOH}$ ) is very attractive, the costs of catalyst and catalyst support [135], the cost of high-quality SSE layer, the cost of high fraction (per kWh) of other inactives (current collectors, separators, electrolyte, gas diffusion layers, packaging, etc.) and the higher cost of “Li–oxygen” cell assembling will never make such cells cost-competitive even with conventional BEV LIBs. This is a strong opinion of the authors, which we share with the community for the sake of completeness and openness. Our opinion, however, should not discourage research community to study this fascinating chemistry for less cost-sensitive applications.

The primary Li sources include lithium chloride ( $\text{LiCl}$ ) – rich brine [138] as well as spodumene ( $\text{LiAlSi}_2\text{O}_6$ ) [139], amblygonite ( $\text{LiAlFPO}_4$ ), petalite ( $\text{LiSi}_4\text{O}_{10}$ ) and other mineral ores [140] (Fig. 6c). The world economic reserves (at the current prices) of Li exceed 31  $\text{Mt}_{\text{Li}}$  [141], which is sufficient to satisfy the EV needs till 2100 and beyond [142]. While the Li price has risen over the past years (currently  $\sim 50$   $\text{\$/kg}_{\text{Li}}$ ), it did not significantly affect cell prices as these comprise less than 2 wt. % Li [20].

### Cost and available reserves of Si

Out of all elements that electrochemically alloy with Li, Si offers by far the best performance characteristics [143,144]. In a fully lithiated (expanded) state Si offers slightly higher volumetric capacity than pure Li ( $2190$   $\text{mAh}\cdot\text{cm}^{-3}$  vs.  $2062$   $\text{mAh}\cdot\text{cm}^{-3}$ ) and the use of Si can prevent formation of Li dendrites (even more so than the use of graphite anodes because of slightly higher lithiation potential of Si and faster rate performance). The volume changes in Si anodes are large, but still much smaller and more controllable than that in Li metal anodes. While some low-performance Si anodes may gradually swell during cycling, the swell in Li metal anodes could be much worse (e.g.,  $\sim 3.8$  times after 200 cycles [124]). In contrast to Li metal plating during charging where precise location of newly deposited Li atoms is virtually impossible to control, the Li alloy formation is limited to the location of Si atoms within the Si anode. So, in this regard, Si anodes serve as a perfect substitute for pure Li anodes with all the benefits that Li brings (high gravimetric and volumetric capacities) but without major Li limitations (formation of dendrites, lack of control and uniformity of deposition, excessive reactivity, etc.). Si anodes could be designed for very rapid charging (e.g., within minutes) at room temperature and could be used in cells exposed to very low temperatures [145,146].

The source of Si is sand ( $\sim 0.01$   $\text{\$/kg}^{-1}$ ), the economic reserves of which are immense [26] (Fig. 6f). Metallurgical grade Si ( $>98.5\%$  Si) and ultra-high purity Si produced for electronic industry and solar cells are costlier ( $0.3$ – $1.5$   $\text{\$/kg}^{-1}$  and  $10$ – $12$   $\text{\$/kg}^{-1}$ , respectively) (Fig. 6g). Formation of composites (Fig. 6h) will increase the anode material cost, but since Si offers  $\sim 10$  times higher gravimetric capacity than graphite, it still offers remarkable value.

### Choice of electrolyte

Commercial LIBs utilize liquid organic electrolytes due to their broad operational temperature, ability to infiltrate into dense electrodes, ability to accommodate volume changes in the electrodes during cycling, light weight, high conductivity, and relatively low cost. However, liquid electrolytes are also known to induce undesirable side reactions with active materials (particularly with conversion-type cathodes) and may form combustible vapors upon battery explosion. To circumvent such limitations, the studies of ceramic solid-state batteries (SSBs) with enhanced electrochemical stability and safety experienced a rapidly growing interest [147]. Yet, ceramic SSBs introduced many new challenges and limitations. The slow interfacial kinetics between many of the solid-state electrolytes (SSEs) and active materials limit rate performance of most SSBs [148]. Low SSE conductivity at low temperatures demands heating of SSBs in cold climates. The poor ability of the ceramic to accommodate volume changes limits the choice of active materials. The commonly poor wettability of the surface of active particles with ceramic SSEs and the high SSE softening temperature makes it challenging to manufacture dense cathodes with high volumetric capacity and low fraction of inactives [128,149]. Being incompatible with conventional LIB factories and commonly requiring moisture-free environment, high temperature and high pressure for the formation of fully dense, mechanically strong solid-state electrodes and cells [150] limits the SSB ability to economically scale to BEV volumes. The high density of SSEs increases the SSB weight. The potential ability of the SSEs to enable dense Li foil anodes [151] is attractive from the volumetric energy density point of view, but is likely not economical for BEVs in the next few decades as we previously discussed. Polymer electrolytes with their much cheaper and easier processing and ability to accommodate larger volume changes may become a more near-term solution (as these can suppress the diffusion of large anionic species such as fluoride-anions and polysulfide-anions to improve stability of conversion-type electrodes [102]), although their electrochemical stability and conductivity need to be further enhanced [152]. As the move from liquid to polymer electrolytes should not change the LIB cost much, we focus on the impact of anode and cathode chemistry in this review.

### Recycling

Over 99% of the lead-acid batteries are recycled in the US [153], and the same is expected for LIBs. However, the economically and environmentally beneficial methodologies for LIB recycling still need to be established. There are three main approaches to recycling LIBs: pyrometallurgical, hydrometallurgical, “mild” methodologies, and their combinations [154]. Pyrometallurgy consists of the high temperature reduction of metal-based compounds to metals along with formation of carbon from organics. Hydrometallurgy involve solution-based processes to leach and precipitate useful compounds. The “mild methodologies” utilize less aggressive thermal treatments to extract metal compounds. Economically, recycling reduces the demands for metals (and thus reduces material costs if recycling levels are substantial,  $>30\%$  [155]), stabilizes supply chain management, and reduces liability associated with old battery storage or utilization costs.

Environmentally, it reduces pollution and human cost accompanying opening new mining operations as well as the emissions associated with the mining and transport of raw materials to distant locations.

### Impact of chemistry on cell-level costs

Slightly over a 50% of an average LIB cell cost comes from the cost of active (anode and cathode powders) and inactive (current collector foils, tabs, binders, conductive additives, separator, electrolyte, case, etc.) materials. As the battery manufacturing technologies improve further in the coming decades, the fraction of materials' related expenses will gradually increase. Fig. 7a shows the contributions to the manufacturing and overheads for a typical cell in 2019: production of electrodes (28%), cell assembling (14%), cell finishing (28%), research and development (R&D) (8%), cost of sales (8%), profit (14%), although there could be meaningful variations within producers. Fig. 7b–d provide more detailed cost contributions for the cell fabrication. Fig. 7e shows the impact of cell chemistry on their 2019 costs. Note that the data we received access to analyzes different large cell manufacturers in Asia and so the age of their cell technology, their manufacturing facilities, the average size of each cell, the average energy density of each cell and the country of origin varies, as indicated. Still, some trends could be distinguished – larger cell energy density typically results in lower cost of inactive materials and lower manufacturing costs. This is because packing more energy in a cell reduces the amount of inactive materials and number of cells that need to be produced per unit energy. However, lower voltage LFP cells may work well with lower cost inactives, are slightly less sensitive to the changes in production environment consistency, resulting in cell cost of only ~\$145 kWh<sup>-1</sup> despite much lower volumetric energy density.

Within a decade or two we expect high capacity Si-based composites will gradually replace graphitic anodes for all cell chemistries. For accurate cell cost predictions, we estimated improvements in energy density because less inactive materials and fewer manufacturing tools would be needed for production of fewer number of higher energy cells needed to attain the same kWh. For the cell energy density assumptions we assumed that average cells attain 70 vol. % energy density of their corresponding battery building blocks (calculating units comprising half of the Al and Cu current collectors' thicknesses, one side of the cathode coating, separator, one side of the anode coating) to take into account packaging, valves, edges, tabs and empty space. This is a simplified (conservative) assumption since larger cells can do better. The current collector foils and automotive separator thicknesses were assumed to remain ~10 μm and ~20 μm, respectively (conservative assumption). Si anodes were assumed to comprise 60 vol. % actives in the lithiated/expanded state (conservative assumption) and have 10% higher areal capacity than cathodes.

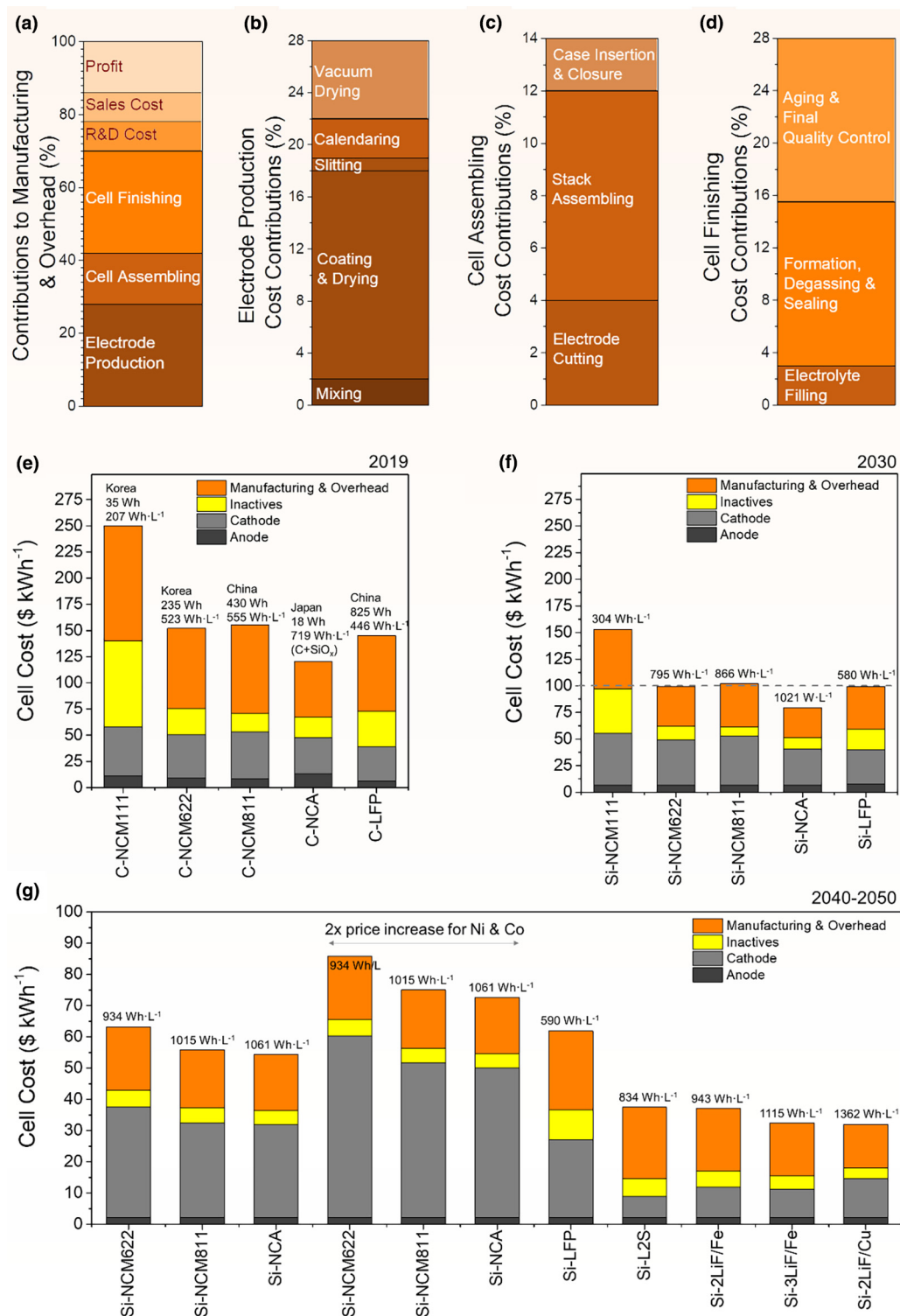
The cell cost values for the tentative year 2030 have been predicted based on the following assumptions: (i) Si composite (with a nominal capacity of ~3000 mAh·g<sup>-1</sup> and cost of ~\$60 kg<sup>-1</sup>) will replace graphite anodes and cathode materials will remain intact in cost and performance (conservative assumption); (ii) for some of the lower energy density cells the areal loading

may increase till the cathode thickness reaches ~100 μm; (iii) the energy-normalized cost of both the manufacturing and the inactive materials will be reduced proportionally to increase in cell energy density and will additionally be reduced by 25% (per cell) due to the expected improvements. Quite remarkably, all the 2030 auto EV cells (apart from NCM111) are expected to become cheaper than \$100 kWh<sup>-1</sup> (Fig. 7f) even considering our conservative assumptions. Note that the energy-normalized cost of the anodes is so small that even if the Si anode price is twice as high (say, \$120 kg<sup>-1</sup>) the cell cost would increase just by ~\$7 kWh<sup>-1</sup> and cells with high Ni/high capacity (>210 mAh·cm<sup>-2</sup>) cathodes (Si/NCA cell in our calculations) would remain sub-\$90 kWh<sup>-1</sup>.

In the longer-term (somewhere between 2040 and 2050) the prospects of EV LIBs become even more exciting (Fig. 7g). For such estimations we assumed that: (i) Si composite cost will be reduced to ~\$20 kg<sup>-1</sup> and the cost of cathode material manufacturing will be reduced to \$2.8–3.7 kg<sup>-1</sup> (half of the 2019 values); (ii) further improvements in cathode packing will further increase the cell-level energy density to the levels estimated assuming all cathodes to be very dense (84 vol.% active for NCM/NCA intercalation-type materials and 74 vol. % active for conversion-type cathodes) and thick (100 μm), (iii) the energy-normalized cost of both the manufacturing and the inactive materials will continue to be reduced proportionally to increase in cell energy density, while further manufacturing technology improvements will reduce the cost of inactives, manufacturing and overhead (per cell volume) to ~50% of the cheapest values found in 2019 cells (by that time, we assume the differences in the costs of inactive and manufacturing will greatly diminish between countries and cell chemistries). As a result of the predicted improvements, all traditional cathode LIB costs will be reduced to \$54–63 kWh<sup>-1</sup>. Unfortunately, at this point the LIB costs become dominated by the cost of NCM/NCA cathode precursors and the probable 2x increase in Ni and Co prices would push the Si–NCM or Si–NCA LIB costs up to \$73–86 kWh<sup>-1</sup>. However, if cheaper conversion-type cathodes are utilized in cell designs without significant sacrifices in the energy density (as in Li<sub>2</sub>S, 2LiF/Fe, 2LiF/Cu or 3LiF/Fe) we expect the LIB cells to remain stable in the \$32–37 kWh<sup>-1</sup> range. Here we assume the conversion cathode material manufacturing costs to be ~2x that of intercalation cathodes (\$6 kg<sup>-1</sup>), but even with ~4x processing cost (\$12 kg<sup>-1</sup>) the Si–3LiF/Fe LIB cost would remain low (\$36 kWh<sup>-1</sup>, estimated).

### Conclusions and outlook

In this article we reviewed the key raw materials' challenges and that are expected to surface in the auto-LIB industry during the next decades, made predictions of their future prices and evaluated new chemistries from the economic points of view. Innovations in manufacturing and chemistry of LIBs have already made them attractive for a broad range of exciting applications, including EVs. Yet, the use of Ni and Co in intercalation-type cathodes and graphite in anodes limit LIB performance and future cost reductions. We discussed why the use of abundant, inexpensive and easy, cheap and safe to mine raw minerals (high grade low-toxicity ores that are cheaper to process) in the composition of

**FIGURE 7**

Impact of active materials' chemistry on the cost of LIB cells: (a–d) cost structure of typical LIB cell manufacturing in 2019; (e) cost structure of averaged LIB cells as a function of cathode chemistry in 2019 (the cell energy and energy density is indicated for completeness); (f) expected auto LIB cell cost in a decade; (g) expected cell cost in over two decades as a function of cell chemistry.

LIB electrodes will become critically important for the transition to near-100% electric transportation. Attaining higher volumetric energy density in future cell chemistry is important for two main reasons: gaining sufficiently long range (provided the volu-

metric constrains of the electric vehicles, busses and trucks to host a battery) and reducing the cell and battery pack costs (as these costs become lower if fewer higher energy cells are used in pack designs). Both evolutionary and revolutionary improve-

ments are expected in all aspects of the battery production for transportation, from pack designs to cell manufacturing to innovations in active and inactive materials. Yet, the transformative move from intercalation-type to conversion-type active materials will be the most instrumental for the transition to low-cost electric transportation. LIB materials already contribute to over 50% of their cost and this fraction is expected to increase further in the coming decades. Material innovations will enable significant savings both directly (by reducing their contributions at the \$/kWh level) and indirectly (by reducing the number of cells of the same size that needs to be built to attain the desired energy). Introduction of conversion-type Si anodes with conventional intercalation-type cathodes within a decade or so should enable high energy density LIB cells to be priced at  $\sim$ \$80 kWh<sup>-1</sup> and in several decades down to  $\sim$ 55 kWh<sup>-1</sup>. However, by that time the LIB price will be largely controlled by the cost of raw materials in the cathodes. The rapidly growing demands for both Co and Ni will quickly outpace their current production capacities, which may induce substantial price volatility even in the near-term (this decade). In addition, the economically viable world reserves for such metals are rather limited and are located outside major LIB consumption areas (North America, Europe, and East Asia), in many cases in countries with poor labor practices such as Congo. As the result of the expected depletion of the high-grade ores and the associated shortages and price increases of Co and Ni in the next few decades may undesirably push the Si–NCM or Si–NCA cell price up to  $\sim$ \$73 kWh<sup>-1</sup> in 2040, which is still not such a bad scenario as it still guarantees transition away from the ICE transportation. On another positive note, the price of less energy dense (smaller range) Si–LFP cells based on abundant metals may become cost-competitive and limit possible price spikes. Finally, with further innovations in conversion-type cathodes as safer, cheaper, more predictable, more sustainable, and more available alternatives, expected LIB cell price down to  $\sim$ 30 kWh<sup>-1</sup> should be attainable by 2040–2050. This should not only accelerate the transition to clean energy in ground transportation, but additionally enable their use in sea and aerial transportation and in electrical grid. The use of such materials will additionally reduce the LIB weight by up to  $\sim$ 3 times, which will benefit weight-sensitive applications. Yet, the development of novel active materials that perform well in real cells, are compatible with existing manufacturing facilities and could be produced economically in huge volumes as well as the subsequent scaling up their production to sufficient volumes will take decades. In particular, conversion-type cathode materials (metal fluorides or Li<sub>2</sub>S-based) need to improve their charge rates, prevent dissolution of active materials during cycling and increase volume fraction of active materials in the electrodes. Conversion-type Si anodes have started to gain commercial traction in the marketplace in 2020, although mostly as additives to graphite-dominant anodes. In addition to energy density increases, the use of thinner Si anodes enables faster charging rates. We expect that the development and scale-up of more electrochemically stable Si-dominant anodes will take over the majority of the market in the next decade or two. At the same time, we strongly believe that due to cost constrains in transportation, the uses of Li metal anodes, “air” cathodes and ceramic SSEs are highly unlikely. The use of solid polymer

electrolytes may become feasible if significant progress is achieved in improving their conductivity and low temperature performance. But even with the success in polymer electrolytes’ development and commercialization, their applications may not meaningfully change cell production costs (even if these remain compatible with conventional tools in LIB factories), although may simplify commercialization of conversion-type cathodes by mitigating their dissolution. Therefore, to warrant a smooth transition to cleaner, energy-sustainable economy it is important to dedicate more efforts to the development of such conversion-type chemistries, which will ultimately lead to the widespread introduction of zero carbon-emission transportation and sustainable energy sources.

### Uncited references

[45].

### Conflict of Interest

G.Y. is a co-founder and stockholder of Sila Nanotechnologies, Inc., the company commercializing Si-based anode materials mentioned in this article.

### Declaration of Competing Interest

The authors declare that they have no known competing financial interests or personal relationships that could have appeared to influence the work reported in this paper.

### Acknowledgements

The authors thank to Army Research Office (grant no. W911NF-17-1-0053) and NASA (grant no. NNX15AP44A).

### Data availability

The raw/processed data required to reproduce these findings cannot be shared at this time due to technical or time limitations.

### References

- [1] A. Manthiram, *ACS Cent. Sci.* 3 (10) (2017) 1063.
- [2] K.C. Divya, J. Åstergaard, *Electr. Power Syst. Res.* 79 (4) (2009) 511.
- [3] J.L. Sullivan, L. Gaines, *Energy Convers. Manage.* 58 (2012) 134.
- [4] O. Schmidt et al., *Nat. Energy* 2 (8) (2017) 17110.
- [5] B. Nykvist, M. Nilsson, *Nat. Clim. Change* 5 (4) (2015) 329.
- [6] C. Vaalma et al., *Nat. Rev. Mater.* 3 (4) (2018) 18013.
- [7] M. Coffman et al., *Transp. Rev.* 37 (1) (2017) 79.
- [8] W. Li et al., *Renew. Sustain. Energy Rev.* 78 (2017) 318.
- [9] O. Edenhofer, *Climate Change 2014: Mitigation of Climate Change*, Cambridge University Press, 2015.
- [10] J. Conti, et al., *International energy outlook 2016 with projections to 2040*; USDOE Energy Information Administration (EIA), Washington, DC (United States). Office of Energy Analysis, 2016.
- [11] D.F. Dominković et al., *Renew. Sustain. Energy Rev.* 82 (2018) 1823.
- [12] M. Winter, R.J. Brodd, *Chem. Rev.* 104 (10) (2004) 4245.
- [13] U. S. A. B. Consortium, *USABC Goals for Advanced Batteries for EVs-CY 2020 Commercialization*.
- [14] Q. Wang et al., *J. Power Sources* 208 (2012) 210.
- [15] F.T. Moore, *Q. J. Econ.* 73 (2) (1959) 232.
- [16] M. Wentker et al., *Energies* 12 (2019) 3.
- [17] N. Nitta et al., *Mater. Today* 18 (5) (2015) 252.
- [18] R. Schmich et al., *Nat. Energy* 3 (4) (2018) 267.
- [19] K. Turcheniuk et al., *Nature* 559 (7715) (2018) 467.
- [20] S. Pacala, R. Socolow, *Science* 305 (5686) (2004) 968.
- [21] M. Wentker et al., *Energies* 12 (3) (2019) 504.
- [22] “This Is What We Die For”: Human Rights Abuses in the Democratic Republic of the Congo Power the Global Trade in Cobalt Amnesty International, 2016.

- 1026 [23] J.F. Thomas Wilson, Bloomberg Technol. (2018).
- 1027 [24] A. Mookherjee, M.K. Panigrahi, J. Geochem. Explor. 51 (1) (1994) 1.
- 1028 [25] A.W. Hofmann, Earth Planet. Sci. Lett. 90 (3) (1988) 297.
- 1029 [26] USCS Mineral Resources Program (2018) <https://minerals.usgs.gov/minerals/pubs/mcs/2018/mcs2018.pdf>.
- 1030 [27] D.T. Allen, N. Behmanesh, Wastes as Raw Materials, National Academy Press, Washington, DC, 1994.
- 1031 [28] G.K.W. Freeman, Process for recovery of cobalt by selective precipitation of cobalt-calcium double salt. Google Patents (2001).
- 1032 [29] The Cobalt Institute (2018) <https://www.cobaltinstitute.org/rechargeable-batteries.html>.
- 1033 [30] J.F. Slack et al., Cobalt, Chapter F of Critical Mineral Resources of the United States—Economic and Environmental Geology and Prospects for Future Supply Professional Paper 1802-F U.S.; 1411339916, US Geological Survey 2017.
- 1034 [31] J.F.E. Slack, U.S. Geological Survey Scientific Investigations Report (2013) 2010-5070-G, p. 218. (<http://dx.doi.org/10.3133/sir20105070g>).
- 1035 [32] G.M. Mudd et al., Ore Geol. Rev. 55 (2013) 87.
- 1036 [33] T.B. Sarah Hannis, Adrian Binks, Cobalt commodity profile, 2009.
- 1037 [34] M.G. Arno, et al., Radiological characterization of a copper/cobalt mining and milling site, in: ASME 2009 12th International Conference on Environmental Remediation and Radioactive Waste Management, (2009), Vol. ASME 2009 12th International Conference on Environmental Remediation and Radioactive Waste Management, Vol. 2, pp. 517.
- 1038 [35] J. Astier, Min. Econ. 28 (1) (2015) 3.
- 1039 [36] R. Sharma, Mar. Technol. Soc. J. 45 (5) (2011) 28.
- 1040 [37] T.A. Schlacher et al., Divers. Distrib. 20 (5) (2014) 491.
- 1041 [38] G.A. Campbell, Miner. Econ. (2019).
- 1042 [39] M. Burton, How the cobalt market fell victim to allure of electric cars. (2019).
- 1043 [40] T. Brown et al., Br. Geol. Surv. (2017).
- 1044 [41] K. Cheyns et al., Sci. Total Environ. 490 (2014) 313.
- 1045 [42] C.L.N. Banza et al., Environ. Res. 109 (6) (2009) 745.
- 1046 [43] R. Sauni et al., Occup. Med. 60 (4) (2010) 301.
- 1047 [44] O. Sachgau, BMW Joins Race to Secure Cobalt for Electric-Vehicle Batteries. (2017).
- 1048 [45] Mineral Commodity Summaries; 2011–2019.
- 1049 [46] G.M. Mudd, Ore Geol. Rev. 38 (1) (2010) 9.
- 1050 [47] M. Elias, Giant ore Deposits: Characteristics, Genesis and Exploration, CODES Special Publication, 2002, p. 205.
- 1051 [48] B. Mishra, Cobalt and nickel production, in: K.H.J. Buschow (Ed.), Encyclopedia of Materials: Science and Technology, Elsevier, Oxford, 2001, p. 1288.
- 1052 [49] N. Campagnol, et al., McKinsey & Company (2017).
- 1053 [50] A. van Bommel, J.R. Dahn, Chem. Mater. 21 (8) (2009) 1500.
- 1054 [51] E.M. Wise, J.C. Taylor, Encyclopaedia Britannica (2015) <https://www.britannica.com/technology/nickel-processing>.
- 1055 [52] H. Hao et al., Energy 101 (2016) 121.
- 1056 [53] B.N.E. Finance, Bloomberg Finance L. P, Tech. Rep (2018).
- 1057 [54] Z. Gao et al., Transp. Res. Rec. 2628 (1) (2017) 99.
- 1058 [55] S. Sripad, V. Viswanathan, ACS Energy Lett. 4 (1) (2019) 149.
- 1059 [56] T. Liu et al., J. Appl. Phys. 115 (17) (2014) 17A751.
- 1060 [57] D. Coutsouradis et al., Mater. Sci. Eng. 88 (1987) 11.
- 1061 [58] G. Harper et al., Nature 575 (7781) (2019) 75.
- 1062 [59] T. Ohzuku, et al., Lithium nickel-manganese-cobalt oxide positive electrode active material. Google Patents (2011).
- 1063 [60] Y. Kim, D. Kim, ACS Appl. Mater. Interfaces 4 (2) (2012) 586.
- 1064 [61] S. Tsubouchi et al., J. Electrochem. Soc. 159 (11) (2012) A1786.
- 1065 [62] J. Jiang et al., J. Electrochem. Soc. 151 (4) (2004) A609.
- 1066 [63] Y. Idemoto et al., J. Power Sources 119–121 (2003) 125.
- 1067 [64] J.M. Lloris et al., Electrochem. Solid-State Lett. 5 (10) (2002) A234.
- 1068 [65] L. Dimesso et al., Solid State Sci. 14 (9) (2012) 1372.
- 1069 [66] D. Choi et al., Nano Lett. 10 (8) (2010) 2799.
- 1070 [67] N. Yabuuchi et al., Proc. Natl. Acad. Sci. 112 (25) (2015) 7650.
- 1071 [68] M. Freire et al., Nat. Mater. 15 (2) (2016) 173.
- 1072 [69] J. Lee et al., Nature 556 (7700) (2018) 185.
- 1073 [70] K. Xu, Chem. Rev. 114 (23) (2014) 11503.
- 1074 [71] C. Li et al., NPJ Comput. Mater. 4 (1) (2018) 22.
- 1075 [72] F. Wang et al., J. Am. Chem. Soc. 133 (46) (2011) 18828.
- 1076 [73] F. Wang et al., ECS Trans. 50 (1) (2013) 19.
- 1077 [74] G.G. Amatucci et al., J. Fluorine Chem. 132 (12) (2011) 1086.
- 1078 [75] F. Badway et al., Chem. Mater. 19 (17) (2007) 4129.
- 1079 [76] P. Poizot et al., Nature 407 (6803) (2000) 496.
- 1080 [77] F. Wu, G. Yushin, Energy Environ. Sci. 10 (2) (2017) 435.
- 1081 [78] H. Li et al., Adv. Mater. 15 (9) (2003) 736.
- 1082 [79] F. Wu et al., Chem. Soc. Rev. 49 (5) (2020) 1569.
- 1083 [80] P.G. Bruce et al., MRS Bull. 36 (07) (2011) 506.
- 1084 [81] J. Xu et al., Nano Energy 51 (2018) 73.
- 1085 [82] J. He, A. Manthiram, Energy Storage Mater. 20 (2019) 55.
- 1086 [83] Q. Pang et al., Nat. Energy 1 (9) (2016) 16132.
- 1087 [84] D. Su et al., Adv. Funct. Mater. 28 (38) (2018) 1870273.
- 1088 [85] J. Dabrowski, Silicon Surfaces and Formation of Interfaces Basic Science in the Industrial World, World Scientific, Singapore River Edge, NJ, 2000.
- 1089 [86] G. Villalba et al., J. Ind. Ecol. 11 (1) (2007) 85.
- 1090 [87] M. Miller, Washington, DC: United States Geological Survey (USGS) (2004).
- 1091 [88] J. Tan et al., J. Power Sources 251 (2014) 75.
- 1092 [89] L. Liu et al., J. Power Sources 238 (2013) 501.
- 1093 [90] M. Tsugenno, et al., Process for producing high-purity silica by reacting crude silica with ammonium fluoride. (1990), Vol. US5458864A
- 1094 [91] 1978.
- 1095 [92] M. Doble, A. Kumar, CHAPTER 14 - semiconductor waste treatment, in: M. Doble, A. Kumar (Eds.), Biotreatment of Industrial Effluents, Butterworth-Heinemann, Burlington, 2005, p. 157.
- 1096 [93] C.-C. Yang et al., J. Iron. Steel Res. Int. 26 (6) (2019) 547.
- 1097 [94] S. Sanghvi et al., RSC Adv. 4 (100) (2014) 57098.
- 1098 [95] J. Aigueperse, et al., Ullmann's Encyclopedia of Industrial Chemistry (2000).
- 1099 [96] N. Pereira et al., J. Electrochem. Soc. 156 (6) (2009) A407.
- 1100 [97] Q. Huang et al., Adv. Energy Mater. 9 (17) (2019) 1803323.
- 1101 [98] W. Fu et al., Adv. Funct. Mater. 28 (32) (2018) 1801711.
- 1102 [99] E. Zhao et al., Adv. Energy Mater. 8 (26) (2018) 1800721.
- 1103 [100] E. Vileno et al., Chem. Mater. 7 (4) (1995) 683.
- 1104 [101] G.G. Amatucci, Nat. Mater. 18 (12) (2019) 1275.
- 1105 [102] Q. Huang et al., Nat. Mater. 18 (12) (2019) 1343.
- 1106 [103] F. Wu et al., Adv. Mater. 31 (43) (2019) 1905146.
- 1107 [104] W. Gu et al., Adv. Energy Mater. 5 (2015) 4.
- 1108 [105] J.K. Ko et al., ACS Appl. Mater. Interfaces 6 (14) (2014) 10858.
- 1109 [106] L. Li et al., J. Am. Chem. Soc. 138 (8) (2016) 2838.
- 1110 [107] A.J. Gmitter et al., Electrochim. Acta 88 (2013) 735.
- 1111 [108] M. Sina et al., J. Phys. Chem. C 119 (18) (2015) 9762.
- 1112 [109] M.A. Reddy et al., Adv. Energy Mater. 3 (3) (2013) 308.
- 1113 [110] S. Kim et al., Adv. Funct. Mater. 27 (35) (2017) 1702783.
- 1114 [111] X. Fan et al., Nat. Commun. 9 (1) (2018) 2324.
- 1115 [112] Q. Huang et al., Small 15 (6) (2019) e1804670.
- 1116 [113] H. Kim et al., Adv. Energy Mater. 5 (2015) 6.
- 1117 [114] R.E. Doe et al., Chem. Mater. 20 (16) (2008) 5274.
- 1118 [115] A.N. Mansour et al., J. Solid State Chem. 183 (12) (2010) 3029.
- 1119 [116] Y. Nishi, Electrochem. Soc. Interface 25 (3) (2016) 71.
- 1120 [117] H. Shi et al., J. Electrochem. Soc. 143 (11) (1996) 3466.
- 1121 [118] T.R. Hupp, et al., Kirk-Othmer Encyclopedia of Chemical Technology (2003).
- 1122 [119] P. Whoriskey, In Your Phone, In Their Air, The Washington Post, 2016.
- 1123 [120] L. Dunner, Br. J. Radiol. 18 (206) (1945) 33.
- 1124 [121] S.R. Gloyne et al., Thorax 4 (1) (1949) 31.
- 1125 [122] B. Liu et al., Joule 2 (5) (2018) 833.
- 1126 [123] R. Weber et al., Nat. Energy 4 (8) (2019) 683.
- 1127 [124] C. Niu et al., Nat. Energy 4 (7) (2019) 551.
- 1128 [125] A.-R.O. Raji et al., ACS Nano 11 (6) (2017) 6362.
- 1129 [126] K. Liu et al., Joule 2 (9) (2018) 1857.
- 1130 [127] J. Janek, W.G. Zeier, Nat. Energy 1 (9) (2016) 16141.
- 1131 [128] K. Kerman et al., J. Electrochem. Soc. 164 (7) (2017) A1731.
- 1132 [129] R.S. Chen et al., Chem. Rev. 120 (14) (2020) 6820.
- 1133 [130] M.J. Du et al., Energy Environ. Sci. 12 (6) (2019) 1780.
- 1134 [131] P. Albertus et al., Nat. Energy 3 (1) (2018) 16.
- 1135 [132] J. Zhang et al., Nat. Commun. 10 (1) (2019) 602.
- 1136 [133] J. Zhang et al., Angew. Chem. Int. Ed. 56 (29) (2017) 8505.
- 1137 [134] W.J. Kwak et al., Chem. Rev. 120 (14) (2020) 6626.
- 1138 [135] P. Tan et al., Appl. Energy 204 (2017) 780.
- 1139 [136] J.-G. Zhang et al., J. Power Sources 195 (13) (2010) 4332.
- 1140 [137] B. Sun et al., Nano Lett. 14 (6) (2014) 3145.
- 1141 [138] G.E. Erickson, R. Salas, U.S. Geol. Surv. Open File Rep. (1987) 88–210, 51.
- 1142 [139] D.C. Yang, Beneficiation of lithium ores by froth flotation. Google Patents (1978).
- 1143 [140] T.E. Dwyer, Recovery of lithium from spodumene ores. Google Patents (1957).
- 1144 [141] S.E. Kesler et al., Ore Geol. Rev. 48 (2012) 55.
- 1145 [142] P.W. Gruber et al., J. Ind. Ecol. 15 (5) (2011) 760.
- 1146 [143] N. Nitta, G. Yushin, Part. Part. Syst. Char. 31 (3) (2014) 317.
- 1147 [144] H. Wu, Y. Cui, Nano Today 7 (5) (2012) 414.
- 1148 [145] H. Wu et al., Nat. Nanotechnol. 7 (5) (2012) 310.

- [146] J. Li et al., *J. Phys. Chem. Lett.* 4 (20) (2013) 3387. 1177
- [147] X. Han et al., *Nat. Mater.* 16 (5) (2017) 572. 1178
- [148] Y. Xiao et al., *Nat. Rev. Mater.* 5 (2) (2020) 105. 1179
- [149] D.H. Kim et al., *Nano Lett.* 17 (5) (2017) 3013. 1180
- [150] J. Auvergniot et al., *Chem. Mater.* 29 (9) (2017) 3883. 1181
- [151] F.D. Han et al., *Nat. Energy* 4 (3) (2019) 187. 1182
- [152] W.E. Tenhaeff, S. Kalnaus, *Handb. Solid State Batteries* (2015) 235.
- [153] L. Gaines, *Sustainable Mater. Technol.* 1–2 (2014) 2.
- [154] C. Liu et al., *J. Cleaner Prod.* 228 (2019) 801.
- [155] J.Y. Mo, W. Jeon, *Sustainability* 10 (2018) 8.